Effects of Symbol Transition Density on Tracking and Acquisition Performance of the Data Transition Tracking Loop at Low Signal-to-Noise Ratios *

S. Million and S. Hinedi
Jet Propulsion Laboratory
California Institute of Technology
4800 Oak Grove Dr., MS 238-343
Pasadena, CA 91109

October 6, 1994

Abstract

Effects of the data transition variation on the performance of the digital data transition tracking loop (DTTL) symbol synchronizer are addressed for symbol SNRs and window sizes of interest. The data transition variation will affect the DTTL performance by introducing an additional timing jitter which results in additional receiver loss. Numerical and simulation results for both tracking and acquisition are presented.

1 Introduction

The symbol synchronizer is the heart of a digital communications system, as it provides symbol timing to many essential components of a receiver. Examples of subsystems that require proper symbol timing for accurate operation include the matched filter, the signal-to-noise ratio (SNR) estimator, the Costas in-phase and quadrature sum-and-dump filters, as well as various baseband lock detectors. In power limited channels, the symbol synchronizer usually extracts the symbol timing directly from the noisy signal [J.], and is appropriately

*The work described in this paper was carried out by the Jet Propulsion Laboratory, California Institute of Technology, under a contract with the National Aeronautics and Space Administration,

termed data-derived symbol sync. Although this method requires no additional power solely for symbol synchronization, the advantage, however, comes at the cost of requiring adequate transtion (zero crossings) in the data symbol sequence. In applications such as Space-to-Earth links, the data transition variation is sometimes very low, and typically additional measures are included in the communications system to guarantee adequate symbol synchronization performance. An example might include randomizing the data stream or using Manchester pulse to guarantee transitions. In applications such as Earth-to-Space links, however, the data stream is not coded to ensure adequate transitions; this is done mainly to simplify the spacecraft complexity. This paper serves to evaluate the tracking and acquisition performance of a commonly used data-derived symbol sync, the digital data transition tracking loop (DTTL), under the environment of data transition variation.

The DTTL symbol synchronizer is used in various receivers such as the Advanced Receiver used by the Deep Space Network [2] and the TDRSS satellite receivers [3]. Its functional block diagram is shown in Fig. 1, and its operation is described below. The baseband input signal is first passed through two parallel channels: the in-phase channel (on top) monitors the polarity of the actual transitions, and the quadrature channel (in the bottom) measures the timing error. Specifically, the in-phase channel accumulates over a symbol followed by a hard decision on the signal polarity. By subtracting two successive decisions, a transition detector is used to determine whether a no' transition (0), a +1 to -1 transition or a -1 to +1 transition occurred. The quadrature channel, on the other hand, accumulates over the estimated symbol transition, and after an appropriate delay is multiplied to the in-phase channel output, I_k. The multiplication results in an error signal, e_k, that is proportional to the estimate of the phase (or timing) error, Subsequently, e_k is multiplied by[1] κ, and then filtered with resulting output being used to control the timing generator.

The performance of the DTTL were first reported in [4-6] assuming equally likely trans-

[1]The factor κ (which is defined later) is used to normalize the error signal so that it is only proportion to the phase difference between the transmitted and received symbol timing.

mitted symbols. Later, the loop performance for an arbitrary transition density was derived in [7] assuming that the noise spectrum of the error signal is independent of the transition density. More recently, the change in noise spectrum was accounted for in [8-9] as well as other effects[2], assuming high symbol SNR and DTTL window of one. The results, nevertheless, were used as approximations for lower symbol SNRS. The steady-state timing jitter given in [9] was simulated in [10], and it was shown therein that at high symbol SNR theory and simulation agree very well, while at low symbol SN R (4 d B or less) theory is more optimist ic than simulation. In this paper, we extend the results of [9] and show the performance of the DTTL taking into account data transition variation for all symbol SNR and window size of interest. We are interested in the low symbol SNR region primarily due to the expected use of higher rate codes (1/4 and 1/6) in future space missions which, consequently, result in lower symbol SNRs.

In the following sections, we determine the performance of the DTTL as a function of data transition variation. In particular, section 2 illustrates the DTTL model, which is used in section 3 to derive the timing jitter. Afterwards in section 4, wc assess the impact of data transition variation on the probability of acquisition, and conclude with the main points of the paper in section 5.

2 The DTTL Model

Consider the DTTL shown in Fig. 1 with a Nonreturn-to-zero (NRZ) signaling format. Assuming that the carrier and subcarrier (if any) have been removed in an ideal fashion, the received baseband waveform is given by

$$r(t) = \sqrt{S}\sum_{k} d_k p(t - kT - \epsilon) + n(t) \tag{1}$$

[2]Data asymmetry, the unequal rise and fall times of the logic gating circuits, also results in additional system loss, but is not considered here.

where S is the data power, T is the symbol time, n(t) is white Gaussian noise with one-sided power spectral density N_o W/Hz, ϵ is the random epoch to be estimated, p(t) is the square- wave function having a value of 1 for $O \leq t <$ T and having value O elsewhere[3], and d_k represents the k-th symbol polarity with p and q representing the *a priori* probabilities of the data d_k taking on values 1 and -1, respectively. The data transition density for a purely random sequence can now be defined as $p_t = 2pq$ which is the measure of the data pattern variation and ranges from zero to 0.5. Let the phase error λ (in cycles) be defined as

$$\lambda \triangleq \frac{\epsilon - \hat{\epsilon}}{T} \tag{2}$$

where ϵ is the received symbol phase and $\hat{\epsilon}$ is the estimated symbol phase. It is clear that the error signal is affected by λ, and in order to quantify this effect, we define the following variables shown in Fig. 2: T is the symbol time; λT is the fraction of the timing error; $\xi_o T$ is the quadrature window; and $R_s = \frac{ST}{No}$ is the symbol SNR. The error signal, e_k, shown in Fig. 2 can now be written as follows

$$\begin{aligned} e_k &= \frac{1}{2}\left\{\sqrt{S}\left[(0.5\xi_o + \lambda)Td_{k+1} + (0.5\xi_o - \lambda)Td_k\right] + V_2 + N_1 + N_2\right\} \times \\ &\quad \operatorname{sgn}\left[\sqrt{S}\left[(1-\lambda)Td_{k+1} + \lambda Td_{k+2}\right] + N_2 + N_3 + V_1\right] \\ &- \operatorname{sgn}\left[\sqrt{S}\left[(1-\lambda)Td_k + \lambda Td_{k+1}\right] + V_1 + V_2 + N_1\right] \qquad \lambda \geq 0 \end{aligned} \tag{3}$$

where sgn[·] denotes the signum function; V_1 and V_2 are the noise components in the k-th symbol; N_1, N_2, and N_3 are the noise components in the (k+1)-th symbol; and W_1 is the noise component in the (k+2)-th symbol as shown in Fig. 2, and they are all independent of each other.

3 DTTL Tracking Performance

One of the key performance measures of the DTTL is the steady-state timing jitter of λ; σ_λ^2. Using linear theory, σ_λ^2 can be derived once the following two quantities are determined:

[3]We assume the DTTL is operating in a wide-band channel so that the received pulses are perfectly square, i.e., no intersymbol interference.

1) the loop S-curve $g(\lambda)$ as a function of the normalized timing λ and 2) the two-sided spectral density S(w, λ) of the equivalent additive noise $n_\lambda(t)$.

The normalized S-curve g.(A) is defined as follows

$$g_n(\lambda) = \frac{\mathrm{g(A)}}{g'(0)_{R_s\to\infty, p_t=0.5}} = \frac{E_{n,s}[e_k|\lambda]}{\sqrt{S}T} \tag{4}$$

where $E_{n,s}[\cdot]$ represents expectation over the signal and noise. The exact closed form solution of $g_n(\lambda)$ can be shown to be [13]

$$g_n(\lambda) = \frac{1}{4}p_t(\xi_o + 6\lambda)\left[\mathrm{erf}(\sqrt{R_s}(1-2\lambda)\right] - \frac{1}{4}p_t(\xi_o - 2\lambda)\left[\mathrm{erf}\left(\sqrt{R_s}\right)\right] \quad \text{for} \quad |\lambda| \le \xi_o/2 \tag{5}$$

where the error function is defined as $\mathrm{erf}(x) = \frac{2}{\sqrt{\pi}}\int_0^x \exp(-v^2)dv$. Fig. 3 shows the normalized S-curve as a function of transition density at low (-5 dB) symbol SNR and it is evident that the average error becomes small as the transition density decreases. This effect is due to most of the I_k values in Fig. 1 being zero as well as the additional noise in the error signal. The first derivative of the S-curve at λ=0, termed the slope of the S-curve, can be shown to be

$$g_n'(0, p_t) = 2p_t\mathrm{erf}\left(\sqrt{R_s}\right) - p_t\xi_o\sqrt{\frac{R_s}{\pi}}\exp(-R_s) \tag{6}$$

which is identical to slope given in *[9]* at high[4] R_s. Fig. 4 shows the slope as a function of symbol SNR and transition density for DTTL window of 0.25. It is evident that at high R_s the slope approaches $2p_t$, but this value drops as R_s decreases.

Assuming that B_LT <<1, it is sufficient to approximate $S(w,\lambda)$, the spectrum of the additive noise $n_\lambda(t)$, at zero frequency; that is, S(O, λ). The normalized noise spectrum can be defined as

$$h(\lambda) = \frac{s(o,\ \lambda)}{\mathrm{S}(0,\ 0)|_{R_s\to\infty, p_t=0.5}} = \frac{s(o,\ \lambda)}{\frac{1}{4}\xi_o N_o T} \tag{7}$$

where S(O, λ) = R(O, λ) + $2R(1,\lambda)$; and R(O, λ) = $E_{n,s}[e_k e_k]$ and $R(1,\lambda) = E_{n,s}[e_k e_{k+1}]$. "In addition, we consider the DTTL only at loop SNR[5] greater that 10 dB, so $h(\lambda)$ is essentially

[4] Observe that erf $\left(\sqrt{R_s}\right) \simeq 1$ and exp $(-R_s) \simeq$ O at symbol SNR greater than 8 dB.

[5] Experience has shown that when the loop SNR, $\rho = \frac{1}{4\pi^2\sigma_\lambda^2}$, is below 10 dB, the loop experiences cycle slipping.

the noise spectral density seen by the loop at $\lambda=0$; that is, h(0). It is shown in [13] that

$$h(0) = 1+p_t\xi_o R_s-\frac{1}{2}(2p_t(R_s\xi_o-2)+2)\,\mathrm{erf}\left(\sqrt{R_s}\right)^2+4p_t\sqrt{\frac{R_s}{\pi}}\exp(-R_s)\left(\mathrm{erf}\sqrt{R_s}+\frac{\xi_o}{\pi}\exp(-R_s)\right)^2 \quad (8)$$

which is the identical to h(0) given in [9] at high symbol SNR and $\xi_o=1$. Fig. 5 shows the normalized noise spectrum as a function of transition density for ξ_o = 0.25. As shown therein, at high symbol SNR h(0) decreases as $2p_t$ while at low symbol SNR h(0) deviates from $2p_t$.

Assuming linear theory, $g_n(\lambda)$ can be approximated as $g_n'(0,p_t)\lambda$ and the variance of λ becomes [1]

$$\sigma_\lambda^2 = \frac{h(0)B_L T\xi_o}{2Rs[g_n'(0,p_t)]^2}\Phi(c) \quad (9)$$

where $\Phi(c)=\frac{B_L^*(c)}{B_L}$, B_L is the design loop bandwidth, and l?;(c) is the actual noise-equivalent loop bandwidth and is defined as [11]

$$B_L^*(c) = \frac{1}{2T}\frac{1}{H^2(1)}\frac{1}{2}\frac{1}{2\pi j}\oint_{|z|=1}H(z)H(z^{-1})\frac{dz}{z} \quad (10)$$

where[6] c is a constant that multiplies λ at the input of the loop filter (i.e., $c\lambda$). The closed loop transfer function $H(z)$ in (11) is given as

$$H(z) = \frac{cF(z)N(z)}{1+cF(z)N(z)} \quad (11)$$

where $N(z)=\frac{T}{z^2(z-1)}$ is the numerically controlled oscillator (N CO) transfer function, and F(z) is the loop filter transfer function: a first order loop filter has a form (Type I)

$$F(z)=4B_L \quad (12)$$

and a second order loop filter has a form (Type II)

$$F(z)=G_1+\frac{G_2}{(1-z^{-1})} \quad (13)$$

[6]The above two-sided complex integral can be evaluated using techniques described in [12].

where $G_1 = rd/T$, $G_2 = rd^2/T$, and $d = 4B_LT/(r - 1)$ with the parameter r typically 2 or 4. For small B_LT products, it shown in [13] for Type I loop filter that $\Phi(c)$ = c while for Type II loop filter $\Phi(c) >$ c. It this paper we present the tracking performance of the DTTL only for a Type I loop filter.

For the DTTL, the S-curve should be normalized by $g_n'(0, p_t)$, so that the loop makes adjustments only to λ. Practically, however, the knowledge of p_t is not available and we must instead normalize the S-curve by $g_n'(0, p_t = 0.5)$, so that the normalization factor in Fig. 1 becomes $\kappa = \frac{1}{g_n'(0, p_t = 0.5)}$. Consequently, the input to the loop filter is $\frac{g_n'(0,p_t)}{g_n'(0,p_t=0.5)}\lambda = 2p_t\lambda$, so that c = $2p_t$. For a Type I loop filter, the timing jitter can be rewritten by absorbing the factor $\frac{g_n'(0,p_t)}{g_n'(0,p_t=0.5)}$ into the the bandwidth, B_L. Disregarding $\Phi(0)$, the variance consequently becomes

$$\sigma_\lambda^2 = \frac{h(0)}{2R_s g_n'(0, p_t) g_n'(0, p_t = 0.5)} \frac{B_{Lo}T\xi_o}{} \qquad (14)$$

where B_{Lo} is the single-sided bandwidth at p_t = 0.5. Note that 'the above variance is identical to that given by Tsang [9] at high symbol SNR, since $g_n'(0, p_t = 0.5) = 1$ in that region. The ratio of the variance given in (9) to that given [9] is plotted as a function of symbol SNR in Fig. 6a. It is clear that at high symbol SNR the two results match as expected while at lower symbol SNR they diverge by as much as 5 dB. Figure 6b, on the other hand, shows the variance as a function of symbol SNR of window size of 1 and 0.25. It is evident that at high symbol SNR the variance is independent of p_t while at low symbol SNR the variance increases for decreasing pt. The dark line in Fig. 6b represent the 10 dB loop SNR threshold and operating above this line can cause cycle slipping. Simulation was conducted to verify the analysis as shown in Fig. 6b for $BLOT$ product of 0.01. Below the 10 dB loop SNR line, simulation and theory agree very well while above it linear theory breaks down, and theory is more optimistic than simulation.

4 DTTL Acquisition Performance

Now that the tracking performance of the DTTL for varying data transition density is characterized, we now investigate its acquisition performance in this environment. Unfortunately, there is no easy way to analytically study the acquisition performance of the DTTL, and we resort to simulation to understand its behavior. Throughout the simulation, a sampling rate of 100 Hz and a symbol rate of 1 Hz are maintained so that there are 100 samples per symbol in each symbol duration. Each simulation was run for $\frac{100}{B_L}$ seconds and if the difference between the ***NCO*** phase and the input phase is with the absolute value of $\frac{\pi}{2}$ for $\frac{10}{B_L}$ seconds (our lock criteria) the simulation stops, and records the normalized time. The simulation was run 200 times for different noise seeds (i.e., different input phases) in order to produce sufficient statistics for the cumulative probability distribution. In the simulation, a type II loop filter with r = 2 was used with B_L=0.0001 Hz and the same NCO transfer function as in the tracking case.

As shown in Figure 7, numerous simulation were run to understand the behavior of the DTTL in the presence of p_t. In particular, Fig. 7a shows the probability of acquisition for $\frac{\Delta f}{B_L}$=0 and 0.25 at a symbol SNR of O dB. Without any frequency offset, the $B_L t$ (acquisition) time for an acquisition probability (P_{acq}) of 9070 is 0.6, 0.8, and 10 for p_t = 50%, 30%, and 10%, respectively. With a frequency offset equal to 0.25 B_L, on the other hand, the $B_L t$ time for P_{acq} = 90% is 0.6, 2, and 20 for p_t = 50%, 30%, and 10%, respectively. It is clear that a frequency offset of 0.25 B_L has little affect on the acquisition time of p_t=0.5. In addition, Figures 7b shows the probability of acquisition for $\frac{\Delta f}{B_L}$= 0,75 again at O dB symbol SNR. We have added the case of $\frac{\Delta f}{B_L}$=0 therein as a reference of comparison. For the $\frac{\Delta f}{B_L}$ =0.75 case, the $B_L t$ time for P_{acq} = 90% is 3.0 and 10 for p_t = 50% and 30%, respectively, while the case for p_t=10% never locks within $\frac{100}{B_L}$ seconds. In general, the acquisition time for p_t=50% is a magnitude lower than p_t=10%, but only slightly less for p_t=30%.

5 Conclusion

This paper presented the tracking and acquisition performance of the DTTL symbol synchronizer under various conditions of transition density and window size. For a Type I loop filter, the tracking performance at high symbol SNR is independent of the transition density, but at low symbol SNR severe degradation can result for low transition density. The acquisition performance of the DTTL was simulated at O dB symbol SNR. As a rough rule, the acquisition time for p_t= 10% is ten times longer than that for p_t=50%.

References

1. W. C. Lindsey and M. K. Simon, *Telecommunication Systems Engineering, New* Jersey: Prentice-Hall Inc., 1973.

2. S. Hinedi, "NASA's Next Generation All-Digital Deep Space Network Breadboard Receiver," *IEEE Trans.* on Common., vol. 41, pp. 246-257, January 1993.

3. "Tracking and data relay satellite system (TDRSS) users' guide" (STDN NO. 101.2), Revision 5, Goddard Space Flight Center, Greenbelt, MD, Sept. 1984.

4. W. C. Lindsey and R. C. Tausworthe, "Digital data-transition tracking loops", Jet Propulsion Laboratory, Pasadena, California, Rep. SPS 37-50, vol. III. pp. 272-276, April, 1968.

5. M. K. Simon, "Analysis of the Steady State Phase Noise Performance of a Digital Data-Transition Tracking Loop" Jet Propulsion Laboratory, Pasadena, California, Space Programs Summary 37-55 vol. 3, pp. 54-62, February, 1969.

6. W. J. Hurd and T. O. Anderson, "Digital transition tracking symbol synchronizer for low SNR coded systems," *IEEE Trans. on Commun. Technology,* vol. COM-18, pp. 589-596, October 1970.

7. T. M. Nguyen and S. Hinedi, "Effects of the Transition Density on the Performance of Data-Derived Symbol Synchronizer," ESA/ESTEC, Noordjwik, The Netherlands, Session 4, pp. 35-51, September 1992.

8. C. S. Tsang and W. C. Lindsey, "Bit synchronization in the presence of asymmetric channel noise," *IEEE Trans.* on *Commun.*, vol. COM-34, pp. 528-537, June 1986.

9. C. S. Tsang and C. M. Chie, "Effect of signal Transition Variation on Bit Synchronizer Performance," *IEEE Trans.* on *Commun.*, vol. 41, No. 5, pp. 673-677, May 1993.

10. S. Hinedi, T. M. Nguyen, and A. Anabtawi, "Minimum Symbol Transition Density on Earth-to-Space Links," Report of the Proceedings of the R and Modulation, Subpanel 1E Meeting at the German Space Operation Center, September 20-24,1993, CCSDS 1320. O-Y-1, Yellow Book, February 1994.

11. S. Aguirre and W. J. Hurd, "Design and Performance of Sampled Data Loops for Subcarrier and Carrier Tracking," *TDA*, vol. 42-79, July-September 1984, Jet Propulsion Laboratory, Pasadena, California, pp. 81-95, November 15, 1984.

12. R. Winkelstein "Closed Form Evaluation of Symmetric Two-Sided Complex Integrals," *The Telecommunications and Data Acquisition Progress Report,* vol. 42-65, July-August 1981, Jet Propulsion Laboratory, Pasadena, California, pp. 133-141, October 15, 1981.

13. S. Million and S. Hinedi, "The Effects of Symbol Transition Density on the Tracking and Acquisition Performance of the Digital Transition Tracking Loop at Low Signal-to-Noise Ratios," to be submitted to *IEEE* Trans. on *Commun.*.

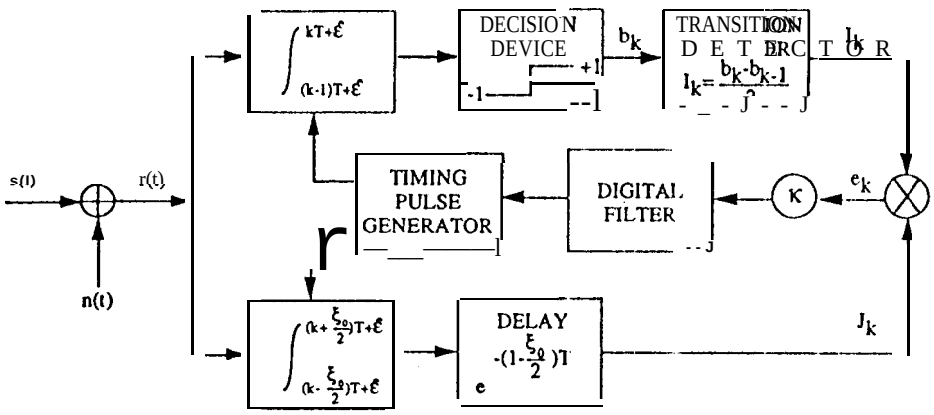

Fig. 1. Digital Data Transition Tracking Loop (DTTL).

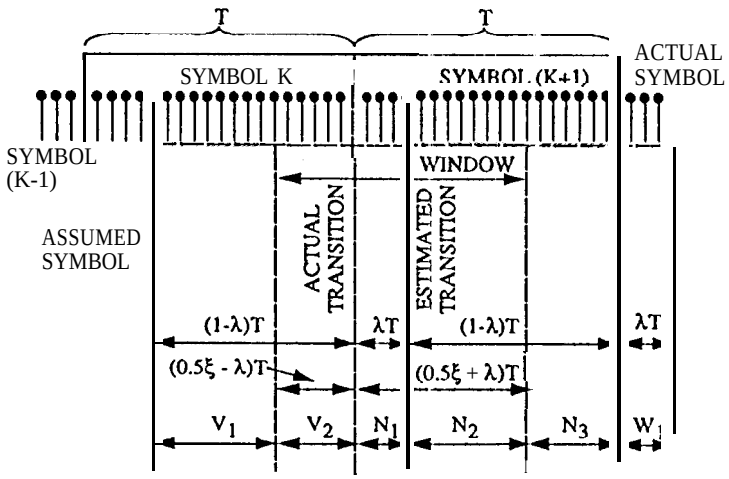

Fig. 2. DTTL model

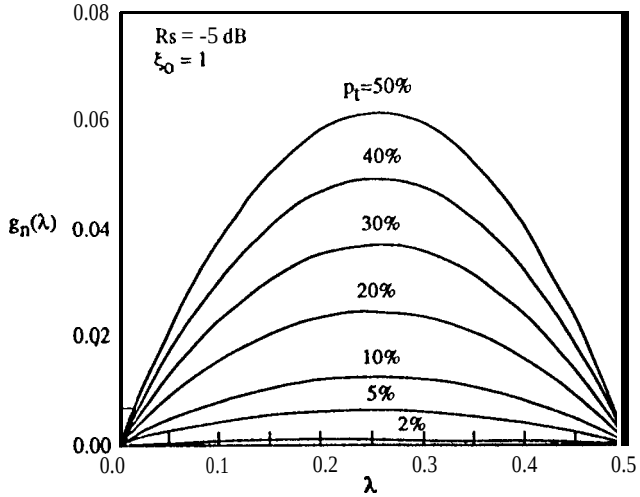

Fig. 3. Normalized S-curve with transition density at Rs = -5 dB

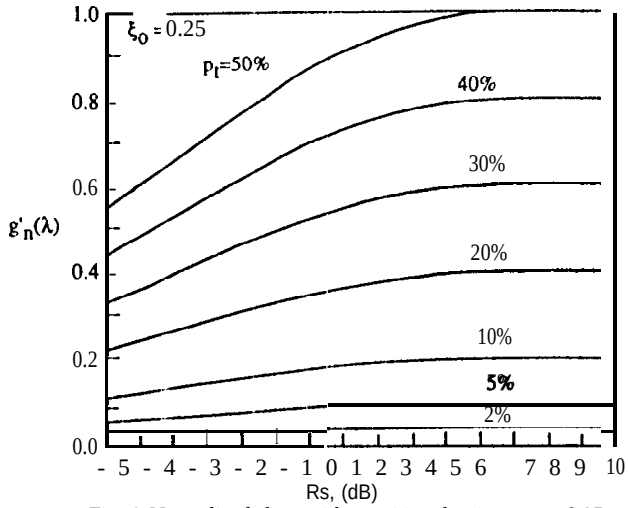

Fig. 4. Normalized slope with transition density at ξ_0 = 0.25

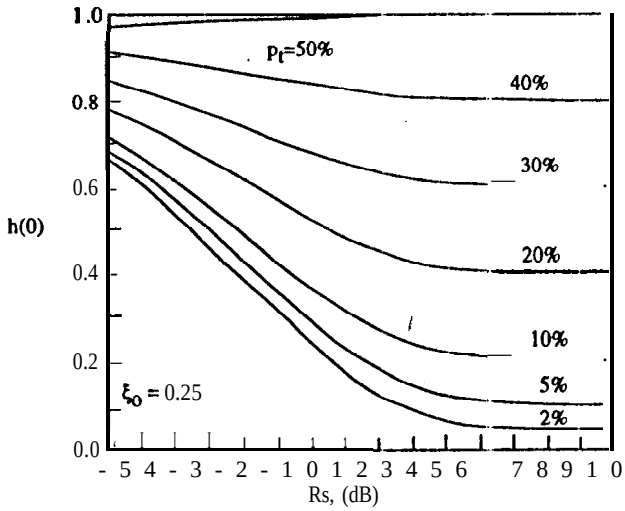

Fig. 5. Normalized noise spectrum at ξ_0 = 0.25

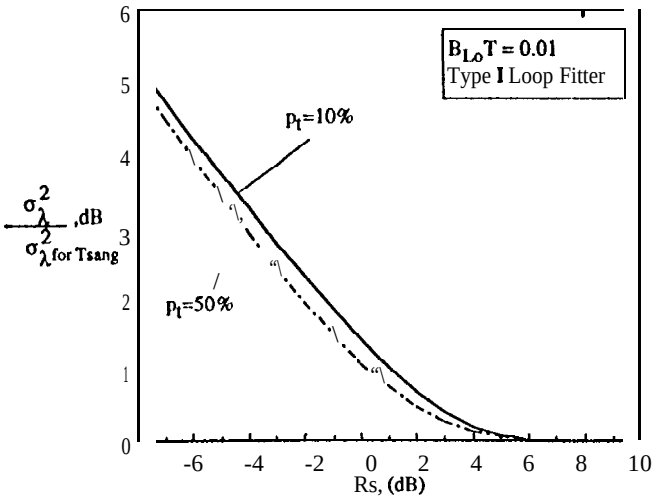

Fig. 6a. The ratio of σ^2_λ given in (9) to σ^2_λ given in [9] vs symbol SNR.

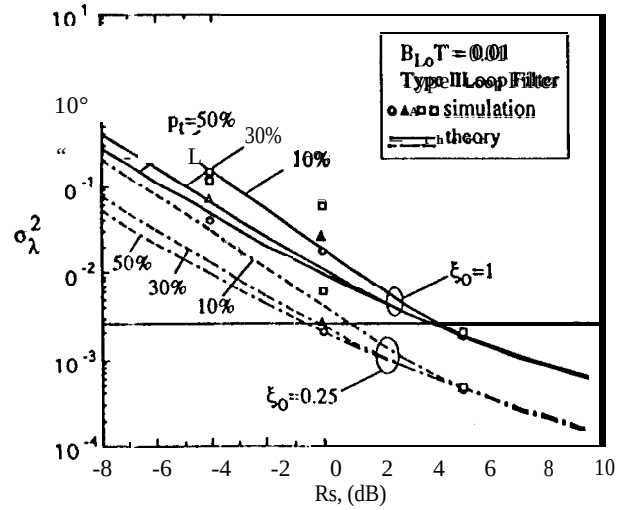

Fig. 6b. Symbol tinting jitter vs symbol SNR for Type II Loop Filter using ξ_0=1 and 0.25.

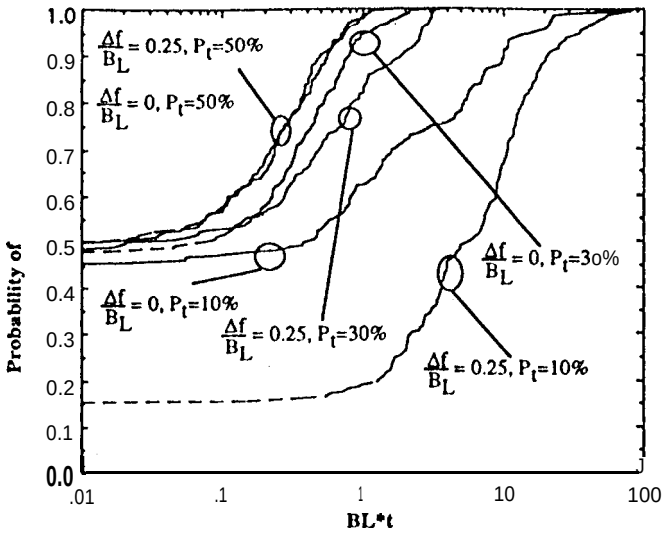

Fig.7a. Probability of Acquisition vs time at R_s=0 dB.

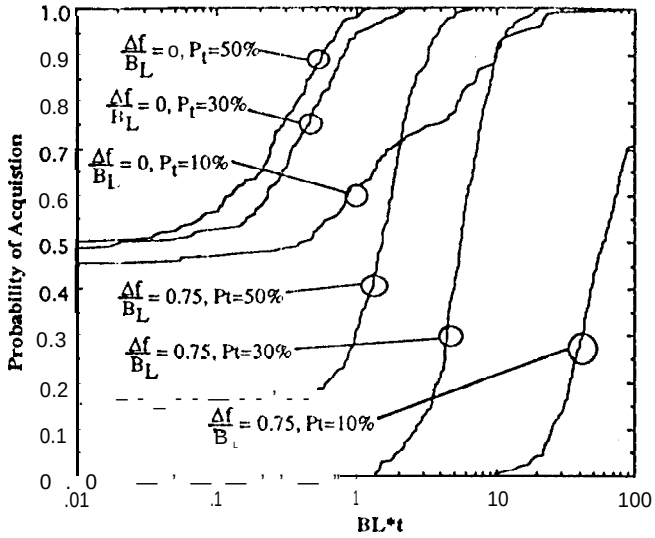

Fig.7b. Probability of Acquisition vs time at R_s=0 dB.